

PACS 61.10.Kw, Nz, 61.72.Dd, Ff, 68.55.Ln

## **Structural changes in Cz-Si single crystals irradiated with high-energy electrons from data of high-resolution X-ray diffractometry**

**I.M. Fodchuk<sup>1</sup>, V.V. Dovganyuk<sup>1</sup>, T.V. Litvinchuk<sup>1</sup>, V.P. Kladko<sup>2</sup>, M.V. Slobodian<sup>2</sup>, O.Yo. Gudymenko<sup>2</sup>, Z. Swiatek<sup>3</sup>**

<sup>1</sup>*Yu. Fed'kovych Chernivtsi National University, Chernivtsi, Ukraine*

<sup>2</sup>*V. Lashkaryov Institute of Semiconductor Physics, NAS of Ukraine, 03028 Kyiv, Ukraine*

<sup>3</sup>*Institute of Metallurgy and Materials Science, Polish Academy of Sciences, Krakow, Poland*

**Abstract.** Structural changes in silicon single crystals irradiated with high-energy electrons ( $E = 18$  MeV) were studied. The peculiarities of diffraction reflection curve behaviour and changes in the profiles of isodiffusion lines in high-resolution reciprocal space maps (HR-RSMs) were found as a function of the radiation dose. The generalized dynamic theory of X-ray Bragg-diffraction in crystals comprising defects of several types (spherical and disc-shaped clusters as well as dislocation loops) and a damaged near-surface layer was used for explanation.

**Keywords:** irradiation, high-energy electrons, Cz-Si, oxygen-containing defects, X-ray diffraction.

Manuscript received 03.02.10; accepted for publication 25.03.10; published online 30.04.10.

### **1. Introduction**

Among the methods of crystal research the methods based on the analysis of the angular distributing of X-ray intensity are the most informative [1-14]. The determination of concentrations and sizes of micro-defects, their type (interstitial or vacancy) and symmetry of static distortion fields formed by them, is possible from the analysis of the angular intensity distributions [3-12].

In the method of X-ray two-crystal diffractometry (TCD) the information about concentration-size descriptions of defects is represented by the tails of diffraction reflection curves, which are mainly formed by X-ray diffuse scattering on microdefects [1-3, 8, 12]. However, only the three-crystal X-ray diffractometry allows to separate diffuse intensity component of X-ray scattering from the coherent one [3-8, 14].

Irradiation of silicon by high-energy particles considerably influences on decomposition processes of oxygen solid solution in Si and, consequently, changes the character of X-ray scattering [9-11]. The presence of a great number of different types of defects in the irradiated samples significantly complicates construction of the model of imperfect structure, allowing to correctly describe the obtained experimental results [15-23].

Therefore, it is necessary to choose the basic types of defects that provide dominant contribution to the diffraction pattern. A similar attempt to construct such a model was undertaken in the papers [9-11], where assumptions of the imperfect system supposing a presence of dislocation loops, ellipsoid clusters ( $\text{SiO}_2$  precipitates), point defects and thermal diffuse scattering in the crystal are used.

The generalized dynamic theory of X-ray Bragg-diffraction in a crystal containing the defects of several types (spherical and disc-like clusters, dislocation loops) was used in this work to research the dynamics of changes of concentration and sizes of dominant defects in crystals before and after irradiation by high-energy electrons as well as their influence on coherent and diffuse components of the diffraction reflection curve.

### **2. Objects of investigations**

They were Czochralski-grown dislocation-free silicon samples (Table 1) irradiated by different doses of high-energy electrons ( $E = 18$  MeV). The oxygen concentration in these samples was  $n \sim 10^{18} \text{ cm}^{-3}$ , input surface orientation (111),  $p$ -type of conductivity, boron-doped, resistivity 7.5 Ohm-cm. To eliminate the damaged layer, crystals prior to and after irradiation were subjected to a complete cycle of chemical and mechanical treatment.

### 3. Experimental investigations

X-ray diffraction curves (Fig. 1) were measured in the  $\omega$ - $2\theta$ -scanning mode with a narrow detector window in common Bragg geometry. The HR-RSMs (Figs 2 and 3) were measured using a triple-axis X-ray diffractometer „PANalytical X’pert Pro MRD XL” in a coplanar diffraction geometry for (333) planes with a rectangular cross-section using 4-fold Ge (220) monochromator and 3-fold Ge (220) analyzer with the angular discrepancy  $12''$ .

**Table 1. Samples under investigation.**

| Sample            | Radiation dose | Thickness, mm |
|-------------------|----------------|---------------|
| N <sub>0</sub> 1  | Reference      | 4.271         |
| N <sub>0</sub> 1a | 1.8 kGray      | 4.263         |
| N <sub>0</sub> 1b | 3.6 kGray      | 4.261         |

Our analysis of experimental data in Fig. 1 shows the following. The crystal N<sub>0</sub>1a (Fig. 1) is characterized by reduction of the full width at half maximum (FWHM) of diffraction curves as compared to the initial sample for both (111) and (333) reflections. Whereas in the case of the crystal N<sub>0</sub>1b for (333) reflection, the situation is opposite. It is caused by different contributions of the damaged near-surface layer to the general scattering intensity for these reflections. Similar peculiarities are observed for rocking curves obtained in the  $\omega$ -scanning mode [3-6].

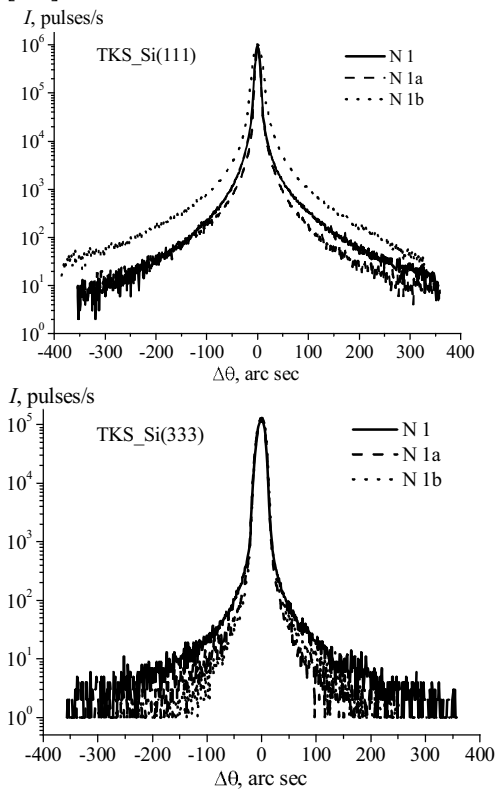


**Fig. 1.** Experimental diffraction reflection curves,  $\omega$ - $2\theta$ -scanning (111) and (333) reflections of  $\text{CuK}\alpha_1$ -radiation. Monochromator – (220).

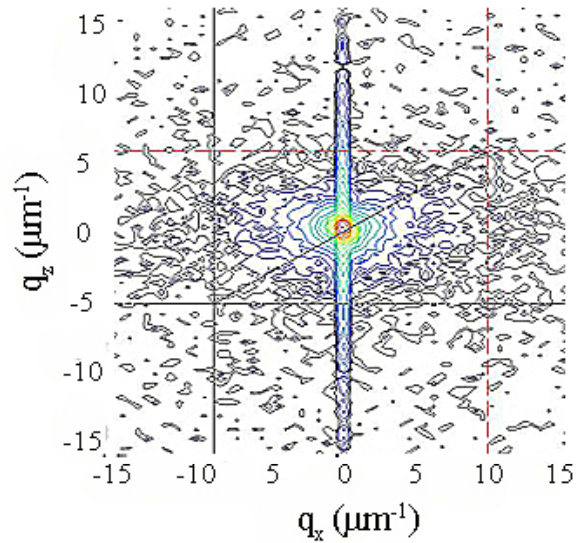


**Fig. 2.** Crystal N<sub>0</sub>1 (reference). Distribution of diffuse scattering intensity around the  $\text{CuK}\alpha(333)$  reciprocal lattice site.

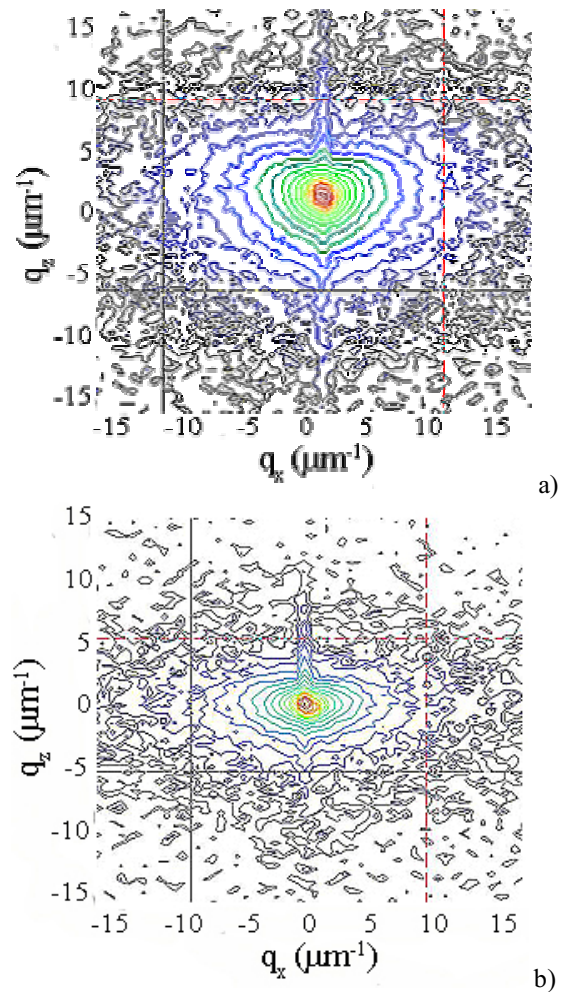


**Fig. 3.** Crystal: a) N<sub>0</sub>1a (1.8 kGray); b) N<sub>0</sub>1b (3.6 kGray). Distribution of the diffuse scattering intensity around the  $\text{CuK}\alpha(333)$  reciprocal lattice site.

In the experimental maps (Figs 2 and 3), the distribution of the diffuse scattering intensity is manifested as certain changes in symmetry of profiles.

It is known that formation of isodiffuse profiles is largely dependent on the type of defects, their location in the lattice and symmetry of their displacement fields [3-8]. General appearance of these profiles allows establishing symmetry of the displacement field and choosing between several possible configurations of a defect structure.

#### 4. Theory

Monocrystalline Cz-Si is characterized by the presence of relatively high concentrations of clusters and dislocation loops. Certain processes, such as temperature annealing, can cause intensive nucleation of new and decay of genetic cluster formations with SiO<sub>2</sub> precipitate structure [12-16]. Based on the evidence from [16-17], the energy of formation of silicon-oxygen precipitates of spherical or elliptical shape is higher than the formation energy of these precipitates in a lamellar or disc shapes, that is, their formation is a most probable [18-22].

However, under certain conditions, for example, high-energy irradiation, different scenarios of defect system reconstruction can occur in bulk silicon crystal. Stimulated diffusion of oxygen from matrix to crystal surface can cause a volume change in the area of precipitate formation. It can account for a nucleation of the dislocation Frank loop [12-16], as well as origination of silicon-oxygen clusters in the (111) planes [16]. Oxygen atoms in these clusters are introduced into interstitial positions between pairs of silicon atoms located along the [111] directions. For a further growth of oxygen-containing clusters, injection of interstitial atoms to surrounding lattice is needed. When concentrations of interstitial atoms in these areas reach a certain critical value, their condensation with formation of the cluster surrounded by a dislocation loop may take place. Such cluster formations have smaller effective sizes than the dislocation loops.

To explain possible structural changes in crystals irradiated with high-energy electrons, we used the following model of interrelated and interacting dominant microdefects typical for Si-Cz crystals [20-22]: disc-like clusters, fine spherical clusters – SiO<sub>2</sub> precipitates, dislocation loops, point defects – silicon vacancies and elastic bend of crystal reflecting (111)-planes.

To determine individual and combined effect of each of the above defect types on the formation of diffraction curves (Fig. 1), we used relationships of the generalized theory of X-ray scattering in single crystals with randomly distributed defects [3-6]. According to this theory, the crystal diffraction curve is a sum of coherent ( $R_{coh}$ ) and diffuse ( $R_{diff}$ ) components [3, 4]:

$$R(\Delta\theta) = R_{coh}(\Delta\theta) + R_{diff}(\Delta\theta). \quad (1)$$

Coherent component is assigned by the relationship [3]:

$$R_{coh}(\Delta\theta) = \left| \frac{\zeta}{L} \right| \left( L - \sqrt{L^2 - 1} \right), \quad (2)$$

where  $L$  is the parameter taking into account absorption of strong Bragg waves due to processes of nonelastic scattering on defects and additional absorption of these waves due to diffuse scattering on defects,  $\zeta$  is the coefficient taking into account dispersion corrections for Fourier-components of polarization  $\chi_H$ .

The diffuse component of reflectivity  $R$  in the presence of several types of randomly distributed defects in crystal and in the absence of correlation between them is of the form [3, 6]:

$$R_{diff}(\Delta\theta) = F_{dyn}(\Delta\theta) \mu_{00}(k_0) t / \gamma_0, \quad (3)$$

$$\mu_{00}(\Delta\theta) = \mu_{DS}(k_0) p(\mu \cdot t),$$

$$p(\mu \cdot t) = (1 - e^{-2\mu \cdot t}) / 2\mu \cdot t, \quad (4)$$

where  $t$  is the crystal thickness,  $\gamma_0$  is the direction cosine of the wave vector of crystal incident wave.

The statistic Debye-Waller factor  $L_H$  and absorption coefficient due to diffuse scattering on defects  $\mu_{DS}$  in  $j$ -layer are a respective superposition on all defect types and described by the expressions:

$$L_H = \sum_{\alpha} L_H^{\alpha}, \quad \mu_{DS} = \sum_{\alpha} \mu_{DS}^{\alpha}. \quad (5)$$

Here,  $\alpha$  is used to number defect type. The factor  $L_H$  in (5) is related to characteristics of dominant defects by the relationships [5]:

$$L_H^D \approx 0.5c\nu_0^{-1}R_0^3(H \cdot b)^{3/2} - \text{dislocation loops,}$$

$$L_H^K \approx 0.5cn_0\eta^2(1 - \eta^2)/100 : (\eta^2 \ll 10) - \text{spherical,}$$

$$L_H \approx cn_0\eta^{3/2} : (\eta^2 \gg 10) - \text{disc-shaped clusters,}$$

where  $c$  is the concentration for the respective type of defects,  $\nu_0$  is the number of atoms in a matrix cubic cell,  $R_0$  is the real defect radius,  $H$  is the vector of reciprocal lattice,  $b$  is the Burgers vector of a dislocation loop,  $n_0$  is the number of cluster-substituted matrix unit cells,  $\eta = \alpha_0 n_0^{1/3} H a_0 / 2 \cdot \pi$ ,  $\alpha_0 = \Gamma \varepsilon R_0^2 h_p / 2$ ,  $h_p$  is the cluster thickness,  $a_0$  is the lattice constant,  $\varepsilon$  is a deformation at cluster boundary,  $\Gamma = (1 + \nu)(1 - \nu)^{-1} / 3$ ,  $\nu$  is the Poisson coefficient.

The coefficient of absorption  $\mu_{DS}$  due to diffuse scattering is described by the relationship [4]:

$$\mu_{DS}^{\alpha}(k_0) = c_{\alpha} C^2(E_j)^2 m_0 J^{\alpha}(k_0),$$

$$m_0 = \frac{\pi \nu_0}{4} (H |\chi_{rH}| / \lambda_c)^2, \quad E = \exp(-L_H), \quad (6)$$

where  $c_\alpha$  is the value of defect concentration in the layer under study,  $C$  is the polarization factor,  $v_0$  is the number of atoms in the matrix cubic cell,  $\gamma_{rH}$  is the real Fourier polarization component,  $\lambda$  is the wavelength,  $J^\alpha(k_0)$  is the normalized coefficient of absorption due to diffuse scattering.

For precipitates that can have the shape of ellipsoids, plates or discs, we have used the relationship between the radius  $R_{d.cl}$  and thickness  $h_{d.cl}$  of disc-shaped precipitate [3, 4]:

$$h_{d.cl} = a_1 R_{d.cl} (L / R_{d.cl})^{a_2}, \quad (7)$$

where  $a_1 = 3.96$  and  $a_2 = 0.5966$  [4]. The parameter of deformation at the interface between the precipitate and Si matrix was assumed to be corresponding to SiO<sub>2</sub> amorphous phase  $\varepsilon = 0.0242$  [3-5].

### 5. Analysis of investigation results

Calculations performed on the basis of relationships (1)-(6) made it possible to reach correspondence between experimental and theoretical diffraction curves (Fig. 4). It allowed evaluation of the sizes and concentrations inherent to dominant types of defects (Table 2).

In particular, a change in the shape of diffraction curve for the crystal №1a (Fig. 1) after following irradiation with high-energy electrons is apparently caused by increase in concentrations of disc-shaped clusters and small-size dislocation loops with a simultaneous decrease in concentrations of fine spherical clusters (Table 2). As a rule, this is reflected accordingly in the essential increase of diffuse component in the integral intensity (Fig. 1).

A slight difference in diffraction reflection curves in Fig. 1 for crystals №1b and №1 (initial sample) can be explained by a decrease in the diffuse intensity component due to reduction in the concentration of disc-shaped clusters and dislocation loops. Also, their size increase with the concentration of fine spherical clusters, which contribution is commensurate to that of disc-shaped clusters and dislocation loops. That is in agreement with the results [8].

**Table 2. Concentrations and sizes of dominant types of microdefects obtained in the process of comparison between experimental and theoretical diffraction reflection curves.**

| Sample | $C_{d.cl.},$<br>$10^6$<br>$cm^{-3}$ | $R_{d.cl.},$<br>$\mu m$ | $C_{L.},$<br>$10^6$<br>$cm^{-3}$ | $R_{L.},$<br>$\mu m$ | $C_{sph.cl.},$<br>$10^{13}$<br>$cm^{-3}$ | $R_{sph.cl.},$<br>nm |
|--------|-------------------------------------|-------------------------|----------------------------------|----------------------|--|----------------------|
| №1     | 15                                  | 3.56                    | 2.5                              | 8.95                 | 19.2                                     | 6.2                  |
| №1a    | 86                                  | 1.8                     | 54.8                             | 7.18                 | 8.16                                     | 5.8                  |
| №1b    | 14                                  | 3.56                    | 9.8                              | 7.2                  | 4.35                                     | 7.9                  |

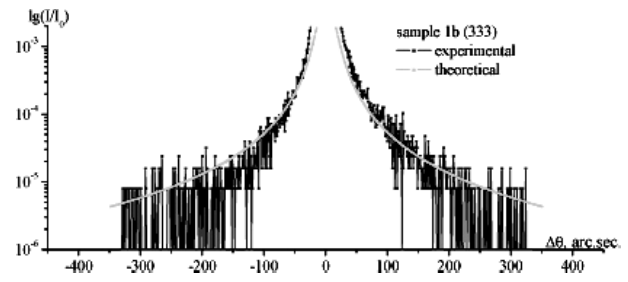


**Fig. 4.** Experimental and calculated rocking curves for the reflection (333) of silicon crystals under study.

The character of scattered intensity distribution in the experimental HR-RSMs (Figs 2, 3) is indicative of the following. The microdefects with a positive power are presented by disc-shaped clusters and fine spherical clusters. The elongated profile of isodiffuse lines in  $q_x$  direction testifies to the presence of prolonged regions of nonuniform composition of oxygen solid solution in silicon with a smeared coherent boundary. In our case, it is interpreted by the Patel model of packing defects [14, 16, 17].

For the crystal №1a (Fig. 3), isodiffuse lines are somewhat smeared and flattened, their curvature radius is increased parallel to  $q_x$  axis. This testifies to a predominant process of increasing the concentration inherent to disc-shaped clusters and small-size dislocation loops on the background of reduced concentrations of fine spherical clusters. Apparently, the energy absorbed in crystal irradiated by the dose of 1.8 kGray is sufficient to cause respective transformations in its defective structure. However, this energy proved to be insufficient to form a stable defective structure relaxed after this high-energy “shock”.

A different situation arises for the crystal №1b. The elliptical shape of profile isodiffuse lines and their elongation in direction of positive  $q_x$  values can bear witness to a reduced concentration of disc-shaped clusters and dislocation loops, and their size increases with the growing concentration of fine spherical clusters.

On the whole, the model of defective structure comprising several types of dominant microdefects yields a more detailed description of the shape and characteristics of diffraction reflection curves, the profiles of isodiffuse lines. This allowed obtaining a scenario of possible structural reconstructions in defective system of silicon crystals irradiated with high-energy electrons [4, 9-11].

### 6. Conclusions

In conformity with the selected model for description of the defective system of Cz-Si crystals by several types of dominant defects, the dynamics of changes in the concentrations and sizes of microdefects prior to and after their irradiation was studied:

- the observed change in the shape of diffraction reflection curves for crystals irradiated by the dose

of 1.8 kGray (sample №1a) with high-energy electrons can be explained by increased concentrations of disc-shaped clusters and small-size dislocation loops on the background of reduced concentrations of fine spherical clusters; slight discrepancies in diffraction reflection curves for crystals irradiated by the largest specific dose 844 Gray/mm (sample №1b) and reference (№1) can be explained by the reduced diffuse intensity component due to a reduced concentration of disc-shaped clusters and dislocation loops as well as their increased sizes with the growing concentration of fine spherical clusters whose contribution is commensurate to that of disc-shaped clusters and dislocation loops.

#### References

1. M.A. Krivoglaz, *Diffuse Scattering of X-rays and Neutrons on Fluctuation Inhomogeneities in Non-perfect Crystals*. Naukova Dumka, Kiev, 1984 (in Russian).
2. A. Authier, *Dynamical Theory of X-ray Diffraction*. Oxford University Press, N.Y., 2001.
3. V.B. Molodkin, A.I. Nizkova, A.P. Shpak et al., *Diffraction of Nanodimensional Defects and Crystal Heterolayers*. Akadempriodika, Kiev, 2005 (in Russian).
4. V.B. Molodkin, V.P. Kladko, S.I. Olikhovskii, E.M. Kislovskiy, T.P. Vladimirova, E.V. Kochelab, R.F. Seredenko, O.V. Reshetnyk, Diffraction characterization of microdefect structure of silicon crystals after isochronal annealing // *Metallofizika i Noveishiye Tekhnologii*, **31**, p. 1205-1222 (2009), in Russian.
5. V.B. Molodkin, S.I. Olikhovskii, E.N. Kislovskii, T.P. Vladimirova, E.S. Skakunova, R.F. Seredenko, B. V. Sheludchenko. Dynamical theoretical model of the high-resolution double-crystal X-ray diffractometry of imperfect single crystals with microdefects // *Phys. Rev. B*, **78**(22), 224109-224121 (2008).
6. V.B. Molodkin, S.I. Olikhovskii, E.G. Len, E.N. Kislovskii, V.P. Kladko, O.V. Reshetnyk, T.P. Vladimirova, B.V. Sheludchenko, Sensitivity of triple-crystal X-ray diffractometers to microdefects in silicon // *Phys. status solidi (a)* **206** (8), p. 1761-1765 (2009).
7. U. Pietsch, V. Holý and T. Baumbach, in: *High Resolution X-ray Scattering from Thin Films and Multilayers*, edited by G. Hoehler // *Springer Tracts in Modern Physics*, vol. 149. Springer-Verlag, Berlin, 1999.
8. V.T. Bublik, S.Yu. Matsnev, and V.Ya. Reznik // Diffuse x-ray scattering study of the formation of microdefects in heat-treated dislocation-free large-diameter silicon wafers // *Fizika Tverdogo Tela*, **45**, p. 1825-1832 (2003), in Russian.
9. V.V. Dovganyuk, I.M. Fodchuk, O.G. Gimchinsky, A.V. Oleinych-Lysyuk, A.I. Nizkova, Determination of dominant type of defects in Cz-Si single crystals after irradiation with high-energy electrons by a change in X-ray reflectivity // *Semiconductor Physics, Quantum Electronics and Optoelectronics*, **9**(2), p. 95-103 (2006).
10. V.V. Dovganyuk, T.V. Litvinchuk, V.V. Slobodjan, I.M. Fodchuk, Defect structure changes in the single Si-crystals after irradiation by high-energy electrons and long natural aging by high-resolution three-crystal X-ray diffractometry // *Proc. SPIE*, **7008**, p. 1B1-1B7 (2008).
11. P. Klang and V. Holý, X-ray diffuse scattering from stacking faults in Czochralski silicon // *Semicond. Sci. Technol.*, **21**, p. 352-357 (2006).
12. L. Capello, T.H. Metzger, V. Holý, M. Servidorio & A. Malachias, Structural properties of ultra-low-energy ion-implanted silicon studied by combined X-ray scattering methods // *J. Appl. Cryst.* **39**, p. 571-581 (2006).
13. V. Holý, Dynamical X-ray diffraction from crystals with precipitates. I. Theory of the Bragg case // *Acta cryst. A* **40**, p. 675-679 (1984).
14. K. Reivi, *Defects and Impurities in Semiconductor Silicon*. Mir, Moscow, 1984 (in Russian).
15. J.R. Patel, Computer-simulation methods in X-ray topography // *Acta cryst. A*, **35**, p. 21-28 (1979).
16. K.F. Kelton, R. Falster, D. Gambaro, M. Olma, M. Cornara and P.F. Wei // *J. Appl. Phys.*, **85**, p. 8097-8111 (1999).
17. W. Patrick, E. Hearn, W. Westdorp, A. Bohg, Oxygen precipitation in silicon // *J. Appl. Phys.* **50**, p. 7156-7164 (1979).
18. H. Bender, Investigation of the oxygen-related lattice defects in Czochralski silicon by means of electron microscopy techniques // *Phys. status solidi (a)*, **86**, p. 245-261 (1984).
19. W. Bergholz, M.J. Binns, G.R. Booker, J.C. Hutchinson, S.H. Kinder, S. Messoloras, A study of oxygen precipitation in silicon using high-resolution transmission electron microscopy, small-angle neutron scattering and infrared absorption // *Phil. Mag. B*, **59**, p. 499-522 (1989).
20. A.J.R. de Kock, Crystal growth of bulk crystals: Purification, doping and defects, in: *Handbook on Semiconductor (vol. 3: Materials, Properties and preparation)*. North-Holland and Publishing Company, 1980, p. 247-333.
21. A.J.R. de Kock, P.J. Roksnoer, P.G.T. Boonen, The introduction of dislocations during the growth of floating-zone silicon crystals as a result of point defect condensation // *J. Cryst. Growth*, **30**(3), p. 279-294 (1975).
22. S. Iida, Y. Aoki, Y. Sugita, T. Abe, H. Kawata, Grown-in microdefects in a slowly grown Czochralski silicon crystal observed by synchrotron radiation topography // *Jpn. J. Appl. Phys.*, **39**, p. 6130-6135 (2000).